Influence of Intermetallic Compounds on RF Resistance of Joints Soldered with Lead Free Alloys

Jiří PODZEMSKÝ, Václav PAPEŽ, Jan URBÁNEK, Karel DUŠEK

Dept. of Electrotechnology, Czech Technical University, Technická 2, 166 27 Prague, Czech Republic

podzejir@fel.cvut.cz, papez@fel.cvut.cz, urbanek@fel.cvut.cz

Abstract. *During soldering process intermetallic compounds as a reaction between solder and substrate are created. Physical properties of those compounds are different to properties of solder and substrate. The influence of intermetallic compounds (IMC) on radio frequency resistance of soldered joints has been identified. Tested solders were lead free Sn-1Cu, Sn-4Ag and Sn-3.8Ag-0.7Cu and lead containing Sn-37Pb (all in weight percent). Samples were annealed up to 3000 hours at 150 °C to accelerate growing of IMC. Radio frequency measuring method has been developed and is described. Influence of IMC on resistance of joint is growing with growing frequency because IMC with slightly different resistivity to base solder is creating barrier to current. Resistance of joints has been measured up to 3 GHz.*

Keywords

RF resistance, intermetallic compounds, lead-free alloys

1. Introduction

Since 2006 the directive on the restriction of the use of certain hazardous substances in electrical and electronic equipment is taking effect in the European Union. The directive names among others lead as an afflicted substance. It had a direct impact on electronic industry because of widely used and proven solder Sn-37Pb. Rapid R&D activities presented large numbers of lead free solders. Properties of the lead free solders are different to lead containing one. Sn-Ag-Cu, Sn-Ag and Sn-Cu families have been taken as the best replacement (the content of Ag varies from 0.35 % to 4.7 % and the content of Cu varies from 0.5 % to 1.7 %) [1].

During soldering process when material of substrate reacts with material of solder products in form of intermetallic compounds are forming. Different solders and substrates create different intermetallic compounds. The formation of IMC on the interface between substrate and solder is necessary for rising well soldered joints with all mechanical and electrical properties. On the other hand, thicker layers of IMCs deteriorate mechanical properties of soldered joints [2]. Except IMC on the interface, others are created in the volume of the solder joints as well. Types and positions of IMC created when solder reacts with copper substrate are listed in Tab. 1.

Sn-Pb		Sn-Ag-Cu		Sn-Ag		Sn-Cu	
type	pos.	type	pos.	type	pos.	type	pos.
Cu_6Sn_5	int.	Cu_6Sn_5	int.	Cu_6Sn_5	int.	Cu_6Sn_5	int.
Cu_3Sn	int.	Cu_3Sn	int.	Cu_3Sn	int.	Cu_3Sn	int.
		Ag_3Sn	vol.	Ag_3Sn	vol.	Cu_6Sn_5	vol.
		Cu_6Sn_5	vol.				

Tab. 1. Types of intermetallic compounds and their positions within the soldered joints. Int. (interface) refers to position between substrate and solder joint, vol. (volume) refers to IMC being created in the volume of the joint [1].

Creation of IMC is explained on the example of SnPb alloy and Cu substrate. After reflow process, a thin layer at the interface is formed thanks to the diffusion of tin in copper and vice versa. The layer is composed of Cu and Sn elements with chemistry Cu_6Sn_5. It has light gray color and melting point 415 °C. Neighboring solder is getting tin-depleted and is getting lead rich which decreases diffusion of tin in copper. Under appropriate conditions (especially at elevated temperature) diffusion of copper in tin continues and results in creation of Cu_3Sn at the interface of copper and Cu_6Sn_5. Cu_3Sn is richer in copper than Cu_6Sn_5, it has dark grey color, melting point around 670 °C and is non wettable [3].

	Cu_6Sn_5	Cu_3Sn	Cu	SnPb	SnAgCu	SnCu	SnAg
Vickers Hardness (kg/mm²)	378	343	50	15	11	14.4	17.9
Young`s Modulus (GPa)	86	108	117	22	31	26	50
Poisson Ration (-)	0.31	0.30	0.34	0.37	0.40	0.12	0.35
Thermal Expansion (10^{-6}/K)	16	19	16	25	21	20	22
Resistivity (µΩ·cm)	17.5	8.9	1.7	14.5	13.0	13.0	12.3
Density (g/cm³)	8.3	9.0	9.0	8.4	7.4	7.3	7.5
Melting point (°C)	415	670	1085	183	216	227	221

Tab. 2. Electrical and mechanical properties of intermetallic compounds, substrate and solders [4] - [7].

Different fragility and electrical resistance of inter-metallic compounds to solder and substrate are most critical mechanical and electrical properties which influence behavior of soldered joints. The overview of selected properties is in Tab. 2. In the paper we focus on changes of resistance of soldered joints under the influence of IMC presence.

2.   Measuring Method

DC electrical resistance of soldered joints is very stable and not influenced by presence of IMC in the joint. DC measuring can be used as a yes/no checking method of testing the quality of final solder joint during manufacturing process. However, DC method is not capable to monitor in detail the quality and especially the internal structure [8]. To get detailed information about quality of soldered joints, RF methods are necessary. There is an existing method which can early detect a predictable open circuit as a result of mechanical stress. The method is based on RF impedance analysis at monitoring frequency between 500 MHz and 4 GHz [9]. The method presented in our paper gives information about resistivity of the solder bulk and the dependency of the resistivity on the amount of IMC presented in the solder bulk. To recognize the influence of IMC high frequency is necessary. The range of our measurement has been considered between 500 MHz and 3 GHz (mechanical size of the sample was a limiting factor).

2.1 Measuring Principle

A measuring head is created as a TEM resonator which consists of a section of an open end coaxial line having electrical length $n \cdot \lambda/2$. The tested sample is a central conductor of the coaxial line. The structure of the resonator in which the central conductor is connected only via capacitive coupling eliminates potential distortion of measured results due to connections. A simple design allows us to easily change tested samples but does not negatively impact measured results. The resistance of the sample can be determined by comparing the quality factor of the resonator with the calibrating central conductor and the measured sample together with a calculation at several resonant frequencies. The quality factor and resonant frequency are measured using amplitude analyzer according to schematics in Fig. 1.
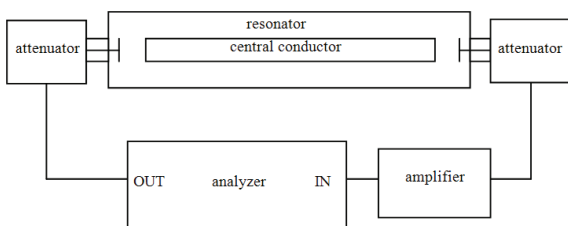

Fig. 1.   Block diagram of the measuring system.

The analysis of the resonator's quality factor is derived from the generalized definition of the quality factor

$$Q_0 = \frac{\omega_r W_a}{P_l} \qquad (1)$$

where Q_0 is the quality factor of the resonator without external attenuation, ω_r is resonant frequency, W_a is accumulated energy in the resonator and P_l is dissipated power in the resonator [10].

Energy stored in the resonator at resonance can be expressed in many ways. The total accumulated energy is generally given by the sum of energy of the electric and magnetic fields. In addition, the total energy is equal to the maximum energy stored in the magnetic field or the maximum energy stored in the electric field in the resonator at resonance. For a TEM wave resonator the energy of the electrical field is given by the equation:

$$W_a = W_{EP} = \frac{1}{2}\int_0^l C'U^2 zdz = \frac{1}{2}C'\int_0^l U_P^2 \cos^2 \beta zdz \quad (2)$$

and by solving the definite integral a simple relationship for stored energy in a resonator can be obtained:

$$W_a = \frac{C'U_P^2 l}{4} = \frac{U_P^2 l}{4Z_0 v_f} \qquad (3)$$

where C' is the capacity per unit length of the line, β is propagation constant, U_P maximum voltage in the resonator, l resonator length, Z_0 characteristic impedance of the resonator and v_f phase velocity of the electromagnetic wave in the resonator.

Without a significant error, the power that is lost in the resonator formed by a section of an "open end" coaxial line having electrical length corresponding to the operational frequency can be approximated with the power dissipated in the resistance of inner and outer conductors of the resonator

$$P_l = \frac{R'}{2Z_0}\int_0^l U_P^2 \cos^2 \beta zdz = \frac{U_P^2 lR'}{4Z_0^2} \qquad (4)$$

where R' is the sum of the resistances of inner and outer conductors of the resonator per unit line length. By substituting (3) and (4) into (1) Q_0 can be expressed as

$$Q_O = \frac{\omega_r l}{Z_0 v_f lR'} = \frac{\pi n Z_0}{R} . \qquad (5)$$

Conductor resistance can be expressed by

$$R = \frac{\pi n Z_0}{Q_0} \qquad (6)$$

where n is the resonator length expressed by the number of half-waves ($\lambda/2$) in the resonator at resonance. The indicated resistance of conductors of the resonator is given by the sum of resistances of inner and outer conductors of the resonator. The skin depth at high frequencies is much smaller than the physical dimensions of the conductor. The resistance for the resonator with inner wire diameter D_1 and

outer tube conductor with inner diameter D_2 can be expressed

$$R = R_1 + R_2 = \frac{l}{\pi D_1}\sqrt{\frac{\omega\mu}{2\sigma_1}} + \frac{l}{\pi D_2}\sqrt{\frac{\omega\mu}{2\sigma_2}} \qquad (7)$$

where σ_1 and σ_2 are conductivities of inner and outer conductors. As the resonator has the constant outer diameter then R_2 is a known function of frequency. The conductivity of the material of the inner conductor (with thickness many times greater than the skin depth) can be expressed by the following equation

$$\sigma = \frac{l^2\omega\mu}{2(R - R_2(f))^2 \pi^2 D_1^2}. \qquad (8)$$

If the inner conductor is non-homogenous (it is made of different materials) then the conductivity is dependent on the ratio between the thickness of the surface layer and the equivalent skin depth and on the conductivity of the surface layer and the core of the conductor. The phenomenon can be described using the current that flows through the conductor and its individual layers. Equation

$$I_1 = \iint_S \sigma_1 E e^{\frac{-\Delta r}{\delta_1}}\, dS = \pi D_1 \sigma_1 \delta_1 E(1 - e^{\frac{-\Delta r}{\delta_1}}) \qquad (9)$$

applies for current flowing through a homogenous conductor where E is the intensity of the electric field on the surface along the axis, according to (7) and (8). Current I_1 flowing through a surface of a composite wire can be expressed as a surface integral of current density on the cross section of the layer (11) and current I_2 flowing through the core can be expressed similarly to the current in a homogenous wire, but with electric field of the same value as electrical field in the surface layer at the interface

$$I_2 = \pi D_2 \sigma_2 \delta_2 E e^{\frac{-\Delta r}{\delta_1}}. \qquad (10)$$

If the conductivity of the materials is known, then after comparing the sum of the currents I_1+I_2 with current I and if $D = D_1 = D_2$ is considered, the surface layer thickness Δr can be expressed by the equation

$$\Delta r = \delta_1 \ln \frac{\sigma_2\delta_2 - \sigma_1\delta_1}{\sigma_e\delta_e - \sigma_1\delta_1} \qquad (11)$$

where σ_e and δ_e are equivalent conductivity and corresponding skin depth.

Reversibly, if the thickness of the surface layer is known, then the conductivity can be determined. Reliable determination of resistance or conductivity of the resonator conductors also crucially depends on the accuracy of determination of the quality factor of the unloaded state resonator. On the resonator, any connection to the outer measuring circuits that diverts energy from it is added to its power loss (1) and therefore creates errors.

The amplitude measurement methodology then shows the quality factor of the loaded resonator Q_Z, which is lower than the quality factor of the resonator in unloaded state [11]:

$$Q_0 = Q_z(1 + \kappa_1 + \kappa_2) \qquad (12)$$

where κ_1 and κ_2 are resonator coupling factors.

The influence of the measuring circuit on the resonator is illustrated in the equivalent circuit according to Fig. 2. The resonator is represented by a parallel resonant circuit consisting of L_r, C_r and G_r. Coupling factor toward the source and the load is assumed to be equivalent and the resonator attenuation caused by the coupling is represented using the same conductivity G. The quality factor of the loaded Q_z and unloaded Q_0 resonator can be expressed using their mutual correlation

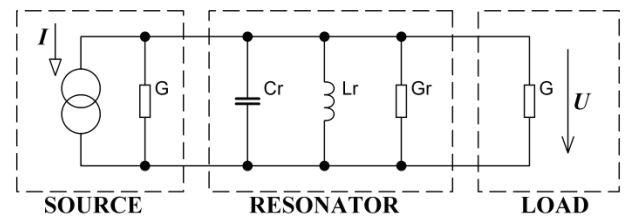$$Q_0 = Q_z(1 + \frac{2G}{G_r}) = Q_z(1 + 2\kappa). \qquad (13)$$

Fig. 2. Principal schematics of the couplings and the resonator.

If the coupling factor is known, then Q_0 can be determined from Q_z according to (13). In practice the calculation is not accurate because the coupling factor comes from another measurement and is also frequency dependent. The only solution is to use very loose coupling, so that the inaccuracy in coupling factor determination causes minimal error for measured value. The complication of this solution is a small power transmission from the source to the indicator. Power transferred from source to load in the circuit in resonance (see Fig. 2) is determined as

$$P = \frac{I^2 G}{(2G + G_r)^2}. \qquad (14)$$

The ratio of the transmitted power P_κ transferred to the load and the maximum power P_0 is given by the equation

$$\frac{P_\kappa}{P_0} = 4(\frac{G}{G_r})^2 = 4\kappa^2. \qquad (15)$$

By comparing (13) and (15), a relationship between achievable transmission of the measuring circuit and measuring accuracy can be determined. The maximum possible measuring error caused by damping of the resonator from external circuits cannot be larger than the root of the number describing the attenuation of the two-port which forms the resonator together with the coupling circuits. If the attenuation is chosen i.e. 40 dB then the maximum value of measurement error caused by attenuation from external circuits is certainly below 1%. A simple correction by the average value of coupling factor lowers this error approximately four times.

3. Experimental Work

3.1 Resonator and Experimental Setup

The resonator was designed to operate in the frequency range from 0.5 GHz to 3 GHz. In this frequency range are up to six resonant frequencies where the conductivity measurement can be done.

The resonator for the measurement is made of OFHC copper. Technical drawing of the resonator is in Fig. 3. Inside the body of the resonator there is a PTFE holder of the inner conductor (tested sample). The holder increases the capacity and losses of the resonator negligibly thanks to its material and the fact that the amplitude of the standing wave in the middle is minimal at certain frequencies. The influence of the holder is further reduced using its special shape – a cylindrical body with thin walls and a large internal cavity.
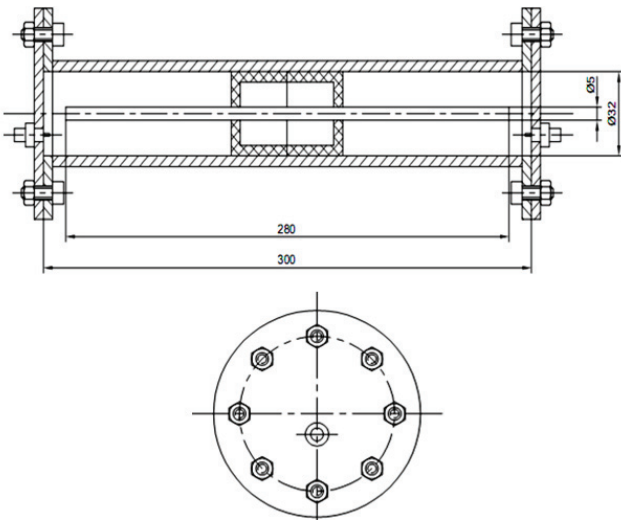

Fig. 3.   Drawing of the resonator.

The central conductor diameter is 5 mm and the diameter of the outer conductor is 32 mm (diameters came out of available semi-finished goods). The mechanical length of the resonating line is 280 mm. The ends of the resonance line are closed; the screws are firmly attached to the flanges that are firmly attached to the outer conductor lines. Simple and robust solution was chosen because the resonator needs to be opened for each measurement and any system that would exhibit any wear during the installation and de-installation would soon be damaged.

The resonator is embedded into the experimental setup (see Fig. 4). We used Agilent network analyzer E5062A which is suitable for frequency range from 300 kHz to 3 GHz.

Both couplings of the resonator in the measuring circuit are designed as capacitive coupling. As the coupling is demanded to be very loose, the coupling capacities are very small and the coupling gates of the resonator are therefore strongly mismatched. Possible resonances and frequency dependence of connected lines are suppressed by attenua-

tion elements (10 dB) which are connected directly to the coupling gates of the resonator.

Fig. 4.   Experimental setup for the measurement of resistance.

The low noise amplifier is used in the circuit due to a relatively large attenuation of the resonator with attenuation elements, (approx. 60 dB to 80 dB) and generally high level of background noise of a network analyzer. The used network analyzer indicates a minimal transmission level of approximately -100 dB in broadband mode with frequency span 2-3 GHz. With the use of a broadband amplifier with a gain of 20-25 dB and noise figure of 2-5 dB, indication of a transmission level of approximately -120 dB is possible.

Using the width of the resonance curve of 3dB the quality factor of the resonator for indicated frequencies is determined. According to the measurement of the reference sample (material of known conductivity σ_1) the resistivity of the outer conductor of the resonator was calculated (it is constant) according to (7). Accuracy of the measuring method was subsequently defined over measurement of other homogenous samples with known conductivity. The result was compared to the value of precise DC measurement which is supposed to define the correct value. The accuracy is in Fig. 5.
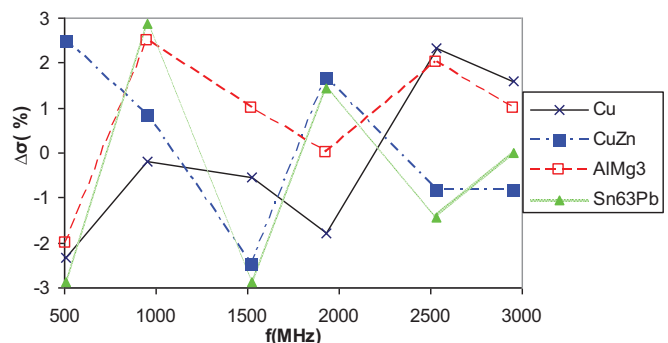

Fig. 5.   Accuracy of RF measuring method of resistivity. Comparison of measured values and target values.

3.2 Sample Preparation

Preparation of the sample was the key issue of the experiment. Although DC measurement of the resistance of soldered joints is quite a simple method, RF measurement is far away from methods applicable for DC measuring. During RF measuring all what comes in the resonator

(electrical component - resistor even with "zero" resistivity, printed circuit board, conducting connections etc.) makes losses. Thus, it would be impossible to identify the real loss of the joint.

To enable RF measurement of resistance of soldered joints and to identify the impact of IMC created on them, the following sample was used. A copper rod (280 mm long, 5 mm diameter) was thermally coated with 15 μm of solders in a special vertical dipping soldering furnace. The layer is thick enough so that thanks to skin effect, current at high frequency will go only through this layer. Its resistivity can be measured with the method described above. On the other hand, the layer is thin enough that a significant part of the solder layer will be transformed to the intermetallic compound in real time under elevated temperature and its impact can be measured.

The tested solders were lead free Sn-1Cu, Sn-4Ag and Sn-3.8Ag-0.7Cu and lead containing Sn-37Pb (all in weight percent). Samples were annealed up to 3000 hours at 150 °C to accelerate growing of IMC. After every 500 hours of annealing time, resistance of the samples was measured, the cross section of the internal structure was observed and the thickness of IMC was measured as well.
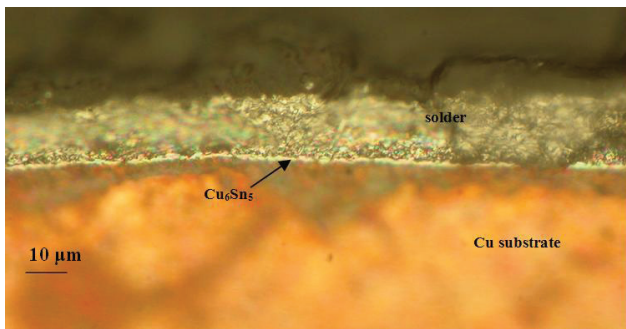

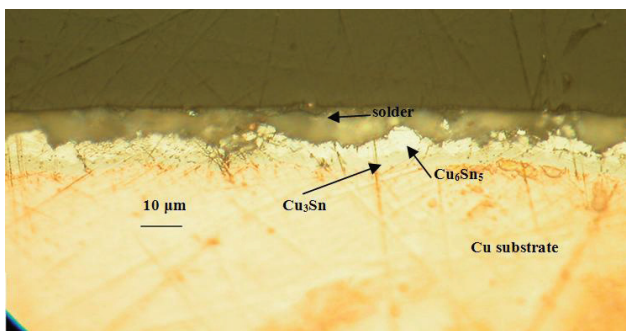**Fig. 6.** Cross section of Sn solder immediately after reflow process.

Fig. 7. Cross section of the annealed sample 1000 hours at 150 °C. The layer of solder is etched out for better distinguishing of IMC from solder.

Cross sections of samples after reflow and annealing clearly show the formation and growing of IMC. In Fig. 6 situation in the joint is obvious. There is just very thin layer of Cu_6Sn_5 IMC at the interface. Dramatic changes are observed after annealing. In Fig. 7 there is a sample annealed 1000 hours at 150 °C. Half of the volume of the joint is

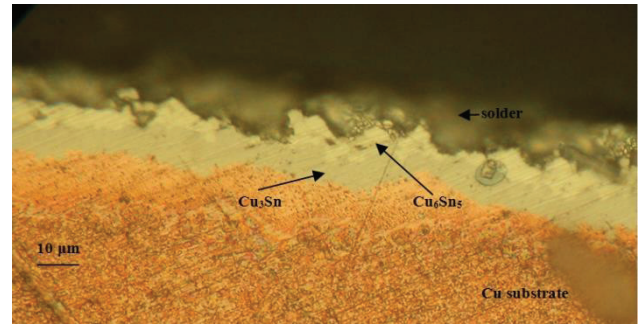transformed from solder to IMC. Cu_3Sn layer is closer to substrate and Cu_6Sn_5 (lighter) is above it.

Fig. 8. Cross section of the sample annealed 3000 hours at 150 °C. The layer of solder is etched out to better distinguish IMC from solder. Cu_3Sn layer (closer to Cu substrate) and Cu_5Sn_6 layer (lighter than Cu_3Sn) are taking significant part of the overall joint.

type	time (h)	Cu_3Sn	$Cu_3Sn+Cu_6Sn_5$	$Cu_3Sn+Cu_6Sn_5+solder$
Sn-3.8Ag-0.7Cu	0	0.0	0.8	17.9
	500	2.5	5.9	18.9
	1000	4.1	8.0	15.6
	1500	4.7	7.9	15.7
	2000	4.7	9.0	18.3
	3000	7.3	14.5	21.2
Sn-4Ag	0	0.0	0.5	15.5
	500	2.5	5.6	16.7
	1000	3.4	7.8	17.2
	1500	4.3	8.6	15.1
	2000	4.0	8.7	14.5
	3000	5.9	12.9	13.9
Sn-1Cu	0	0.0	0.8	16.4
	500	2.8	6.2	13.6
	1000	4.1	8.7	17.1
	1500	4.2	9.7	16.7
	2000	5.0	10.6	15.3
	3000	8.2	16.2	19.5
Sn-37Pb	0	0.0	0.5	15.7
	500	3.5	7.8	14.8
	1000	4.7	9.2	22.2
	1500	6.2	10.0	11.3
	2000	7.3	10.8	14.5
	3000	9.6	9.9	12.0

Tab. 3. Overview of measured thickness of intermetallic compound layers Cu_3Sn and Cu_6Sn_5 for each tested solder after different annealing time.

Measured thickness of IMC is in Tab. 3. There is a listed thickness of Cu_3Sn, total thickness of both layers

Cu_3Sn plus Cu_6Sn_5 and total thickness of both IMC layers plus resting solder layer.

frequency (GHz)	skin depth (μm)			
	SAC	SnAg	SnCu	SnPb
0.5	8.12	7.91	8.12	8.57
1	5.74	5.59	5.74	6.06
2	4.06	3.95	4.06	4.28
3	3.31	3.23	3.31	3.50

Tab. 4. Skin depth of tested solders within the range of frequencies.

Skin depth for tested solders within the measured frequency range is in Tab. 4. Typical roughness of the surface of tested rods is in Fig. 9 with $Ra = 0.37$ μm.
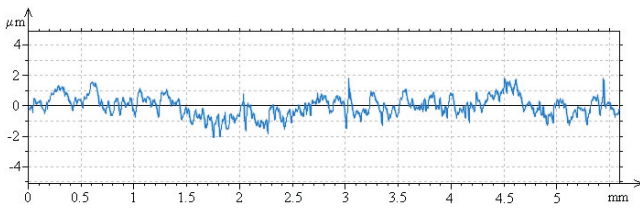
Fig. 9. Typical roughness of surface of measured rods. Roughness was measured along the axis of the rod.

3.3 Measuring of Resistance

Measuring of resistance of samples was done after reflow process and then every 500 hours of annealing at 150 °C up to 3000 hours in total.
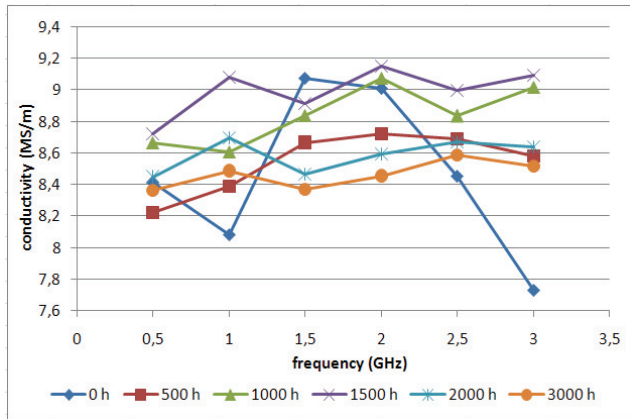
Fig. 10. Changes of conductivity of solder joint made of Sn-3.8Ag-0.7Cu solder at frequency range from 500 MHz up to 3 GHz for annealing up to 3000 hours at 150 °C.

In figures describing changes of conductivity of soldered joints depending on annealing time (Fig. 10 - Fig. 13) we can see that general trend has decreasing tendency. It supports an idea that IMC is influencing the resistivity as it is creating certain barrier to flowing current. Dependency of conductivity on frequency is not as dramatic as dependency on annealing time but we can see certain growing tendency of conductivity with higher frequency. The reason

of that dependency can be connected to skin depth. At higher frequencies skin depth is smaller which in case of our soldered joints means that current is going via an area where the original solder (still not transformed to IMC) is.
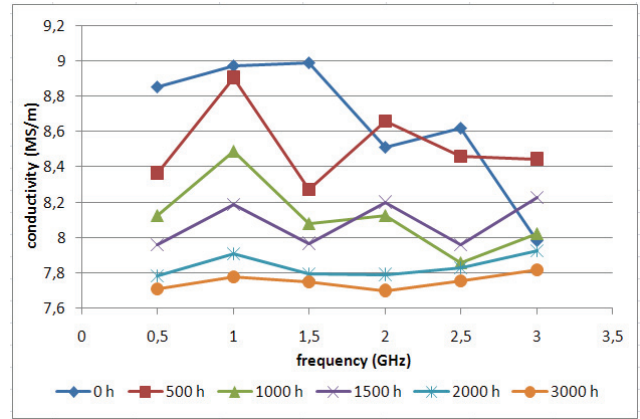
Fig. 11. Changes of conductivity of solder joint made of Sn-4Ag solder at frequency range from 500 MHz up to 3 GHz for annealing up to 3000 hours at 150 °C.

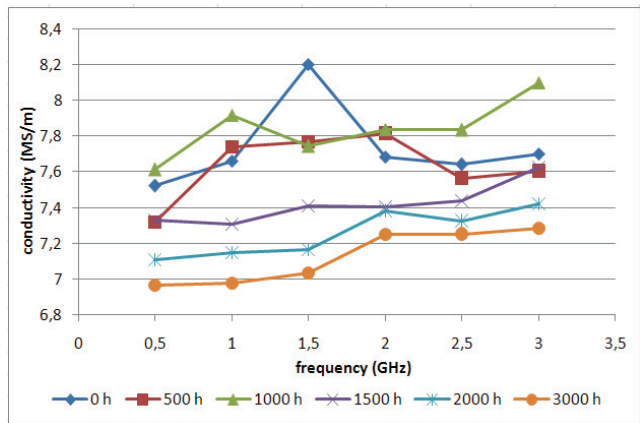**Fig. 12.** Changes of conductivity of solder joint made of Sn-1Cu solder at frequency range from 500 MHz up to 3 GHz for annealing up to 3000 hours at 150 °C.
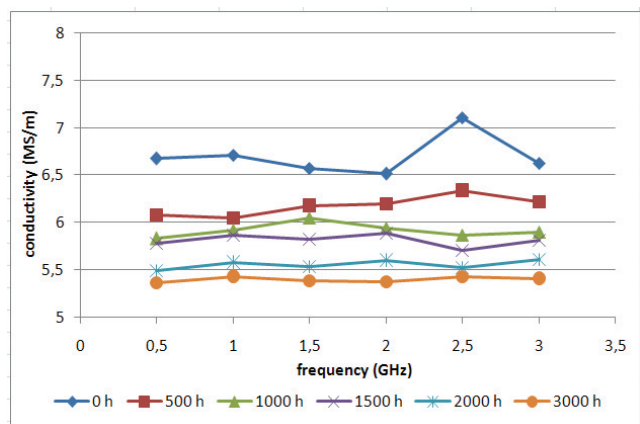
Fig. 13. Changes of conductivity of solder joint made of Sn-37Pb solder at frequency range from 500 MHz up to 3 GHz for annealing up to 3000 hours at 150 °C.

4. Conclusion and Discussion

The goal of the paper is to describe the developed method of measuring RF resistance of soldered joints. It allows us to measure RF resistance within the range of frequencies from 500 MHz to 3 GHz. The method is accurate enough to provide us with relevant data. The accuracy of the method is ±3 % within frequency range stated above.

The RF resistivity of soldered joints has been measured and the influence of presence of created intermetallic compounds has been observed.

Presence of IMC differs between types of solder. If we consider total initial thickness of solder vs. total thickness of created intermetallic compound as an assessment factor than solder Sn-4Ag would be considered as the worst one (the solder with higher creation of IMC). The second worst would be Sn-1Cu followed by Sn-37Pb. Solder Sn-3.8Ag-0.7Cu comes from the comparison as the least vulnerable to IMC creation.

The result of assessment of IMC creation corresponds to the result of changes of RF resistance of soldered joint. Having a look at difference between values of non annealed sample of joint made of Sn-4Ag and annealed one at frequency 500 MHz we compare conductivity 8.8 MS/m with 7.7 MS/m which is difference of 12.5 %.

Presence of intermetallic compounds in the soldered joint influences its resistivity especially at high frequency. The drop of resistivity we measure is between 10 % and 15 % of value of resistivity of joints without significant presence of intermetallic compounds.

Acknowledgements

References

[1] HWANG, J. S. *Environment Friendly Electronics: Lead Free Technology*. Electrochemical Publications Ltd., 2001.

[2] PODZEMSKÝ, J., URBÁNEK, J., DUŠEK, K. Shear test of joints made of lead free solders. In *Proceedings of 34th International Spring Seminar on Electronics Technology*. Tatranska Lomnica (Slovakia), 2011, p. 84 - 88.

[3] KLABAČKA, E., URBÁNEK, J. *Technology of Electronic Instruments (Technologie elektronických zařízení)*. Vydavatelství ČVUT, 1997 (in Czech).

[4] FIELDS, R., LOW, S. Physical and mechanical properties of intermetallic compounds commonly found in solder joints. In *Proceedings of TMS Symposium*. Cincinnati (USA), 1991.

[5] National Institute of Standards and Technology. *Database for Solder Properties with Emhpasis on New Lead-free Solders* (web page). [Online] Cited 2012-01-05. Available at: http://www.boulder.nist.gov.

[6] YAMAMOTO, T., TSUBONE, K. Assembly technology using lead-free solder. *FUJITSU Scientific & Technical Journal*, 2007, vol. 58, p. 50 - 58.

[7] UCLA Engineering, USA. *Recent Progress in Lead (Pb) Free Solder and Soldering Technology (presentation)*. 15 pages. [Online] Cited 2012-04-14. Available at: http://www.seas.ucla.edu /ethinfilm/Pb-freeWorkshop/pdf/kang.pdf.

[8] ĎURIŠIN, J. Properties of joints made of lead free alloys (Vlastnosti spojov na báze bezolovnatého spájkovania). The Technical University of Košice, Košice (Slovakia), 2009. *Doctoral thesis* (in Slovak).

[9] KWON, D., AZARIAN, M. H., PECHT, M. G. Detection of solder joint degradation using RF impedance analysis. In *Proceedings of 58th Electronic Components and Technology Conference*. Florida (USA), 2008, p. 606 - 610.

[10] KUMMER, M. *Basics of Microwave Engineering* (Grundlagen der Mikrowellen-technik). VEB Verlag Technik, 1989 (in German).

[11] TISCHER, F. J. *Microwave Measurement (Mikrowellenmeßtechnik)*. Springer-Verlag, 1958 (in German).

About Authors ...

Jiří PODZEMSKÝ was born in 1983 in Most, Czech Republic. He received his M.Sc. in Electrical Engineering in 2008 from the Czech Technical University in Prague, Faculty of Electrical Engineering. His research interests include mainly soldering and other processes related to electrotechnology. He is currently a postgraduate student and his work is focused on degradation of soldered joints made of lead free alloys.

Václav PAPEŽ was born in 1954 in Prague, Czech Republic. He received his M.Sc. degree and the Ph.D. degree in Radio Electronics from the Czech Technical University in Prague, Faculty of Electrical Engineering in 1979 and 1984, respectively. He is currently an associate professor at the Department of Electrotechnology, Czech Technical University in Prague. His research interests are in the field of radiowave propagation and power electronics.

Jan URBÁNEK was born in 1939. He received his M.Sc. degree and the Ph.D. degree from the Czech Technical University in Prague, Faculty of Electrical Engineering. He is currently an associate professor at the Department of Electrotechnology, Czech Technical University in Prague. His research interests are in the field of soldering in electronics and issues related to lead free soldering.

Karel DUŠEK was born in 1978. He received his M.Sc. degree and the Ph.D. degree from the Czech Technical University in Prague, Faculty of Electrical Engineering. His research interests are in the field of lead free soldering with focus on analysis of surface of soldered joint.